



Contents lists available at ScienceDirect

Tetrahedron

journal homepage: www.elsevier.com/locate/tet

Long-wavelength boradiazaindacene derivatives with two-photon absorption activity and strong emission: versatile candidates for biological imaging applications

Dakui Zhang^a, Yaochuan Wang^b, Yi Xiao^{a,*}, Shixiong Qian^{b,*}, Xuhong Qian^{c,*}^aState Key Laboratory of Fine Chemicals, Dalian University of Technology, Zhongshan Road 158, Dalian, China^bPhysics Department, Fudan University, Shanghai, China^cShanghai Key Laboratory of Chemical Biology, East China University of Science and Technology, Meilong Road 130 Shanghai, China

ARTICLE INFO

Article history:

Received 24 June 2009

Received in revised form 31 July 2009

Accepted 3 August 2009

Available online xxx

Keywords:

BODIPY dyes

NIR emission

Two-photon absorption

Bioimaging

ABSTRACT

Novel D π D type boradiazaindacene dyes exhibit considerable two photon absorption cross section and strong red emission. Cell stained with these dyes show bright intracellular fluorescence. These properties qualify them as competitive candidates for fluorescent bioimaging applications

© 2009 Published by Elsevier Ltd.

1. Introduction

Fluorescent imaging at the cellular and subcellular levels within a living organism is a powerful tool for life sciences.¹ As the fluorescent reporters, organic dyes will not significantly influence the biological functions on account of the small molecular sizes. Although there are a large number of fluorescent organic compounds, only a few can satisfy the fundamental requirements such as high fluorescence quantum yields, large molar extinction coefficients, large Stokes shifts, high photostability, etc. Moreover, almost all these frequently applied fluorescent dyes absorb and emit relatively short wavelength light, which has poor tissue permeability, may cause photodamages, and is easily interfered by biological self fluorescence.² The scarcity of excellent fluorophores in the long wavelength region has become one of the major obstacles for imaging in vivo. Although some conventional near infrared (NIR, 650–900 nm) dyes, e.g., cyanines, have been adopted temporarily, their future applications are problematic due to the drawbacks, such as low fluorescence quantum yields and poor photostability.³

On the other hand, microscopies based on two-photon excited fluorescence (TPEF) represent a new emerging and important tendency in fluorescent imaging. This technique provides some

advantages such as the capacity for a highly spatially confined excitation and intrinsic three-dimensional resolution, the ability to image at an increased penetration depth in tissue with reduced photodamage and background fluorescence by operating with excitation radiation in the NIR region.⁴ However, only few conventional fluorescent dyes, such as rhodamines, exhibit enough two-photon absorption (TPA) cross sections for practical application in two-photon bioimaging. Thus, there has been a lot of research focused on the development of new fluorophores with large TPA cross sections as well as high fluorescence quantum yields.⁵ To date, TPEF peaks of the new fluorophores are generally located in the 400–600 nm region. Even they can be excited by NIR laser, the short wavelength of emission remains an unsolved problem, which lowers their competitiveness to conventional NIR dyes (both excitation and emission are in the NIR region). To obtain materials with combined advantages of two-photon absorption activity and red even longer emission, many efforts have been paid out.⁶ Prasad and co-workers suggest a FRET (fluorescence resonance energy transfer) strategy.⁷ They utilized efficient two-photon fluorophores as energy donor and connected them to the long wavelength dye (without TPA activity) as the acceptor. Upon two-photon excitation of the donor, FRET proceeded efficiently and resulted in acceptor's emission. This idea is creative and enlightening. The only problem is that such FRET molecules are complicated and difficult to synthesize.

The goal of this investigation is to develop versatile fluorophores suitable for both single and two-photon microscopic imaging.

* Corresponding authors. Tel.: +86 411 39893870; fax: +86 411 83673488.

E-mail address: xiaoyi@chem.dlut.edu.cn (Y. Xiao).

Clearly, they should feature the integrated characteristics of considerable two photon absorption across sections, long wavelength region (>650 nm) emission, high fluorescence quantum yields, and good photostability, facile synthesis, etc.

2. Results and discussions

4,4-Difluoro-4-bora-3a,4a-diazasindacene (BODIPY) dyes have been widely used as bioimaging fluorescence dyes⁸ due to their excellent optical properties.⁹ However, to our knowledge, there were only few reports about the BODIPY dyes' two-photon absorption related properties, which were, generally, unsatisfactory.¹⁰ Some of them have short TPEF wavelengths.^{10a–e} Although some others were designed to have enlarged conjugation and strong ICT (intramolecular charge transfer) nature, they do not show any TPA activity.^{10c} Only a very recent paper reported novel BODIPY derivatives with long wavelength absorptions and large TPA cross sections, but it didn't mention their emission properties.^{10f}

According to experiences, introducing substituents on 2,6 positions of BODIPY core will influence the spectra remarkably and obtain quite symmetrical structure.¹¹ According to the literature,^{5a,c,12} efficient ICT processes and D- π -D structures are important factors in designing two-photon absorption molecules. The linear and symmetrical configuration would be more beneficial for charge transfer process, which was a favorable factor for obtaining good TPA properties.

We expected that a strong red emission by direct two-photon excitation would be achieved by using the strong fluorescent BODIPY dyes. In the D- π -D type (Donor- π -bridge-Donor) dyes **3b** and **3c**, a central BODIPY core with a considerable electron-accepting nature was connected with the triphenylamino or carbazole groups. For an ICT process to occur, an efficient π -conjugated spacer is required to facilitate the electronic flow. Ethynyl is a popular spacer for two-photon chromophore design. Sometimes, efficient ICT process can also cause strong red emission.¹³

We efficiently introduced π -electron donors into 2,6 positions of the BODIPY core via Sonogashira coupling reaction to increase the absorption and emission wavelength as shown in Scheme 1. Iodination of the precursor BODIPY **1** with excess *N*-iodosuccinimide (NIS) gives the 2,6-bisido BODIPY **2** in high yield (85%) while the aromatic alkynes in compounds **3b** and **3c** were synthesized via a few steps from the start materials (details in Supplementary data). Sonogashira coupling reaction of 2,6-bisido BODIPY **2** and the alkynes produced compounds **3b** and **3c** with satisfactory yields 75% and 68%, respectively.

All the linear and nonlinear properties were studied in THF solution, and are summarized in Table 1. The normalized spectra are depicted in Fig. 1. The absorption and emission wavelength of **3b** and **3c** are longer than those of **3a**, which is a reference compound

because of the strength of electron-donating groups. Comparing compounds **3b** and **3c** with **3a**, an increase of the Stokes shift and the half-bandwidth of the fluorescence spectra are observed. Such behavior is indicative of charge redistribution occurring upon excitation, prior to emission, and potentially large TPA cross section.^{5c}

Table 1
One- and two-photon properties of compounds **1** and **3a–3c** in THF

Compound	λ_{SPA}^a nm	λ_{SPEF}^b nm	Δs^b nm (cm ⁻¹)	ϕ^c	λ_{TPE}^d nm	σ^e GM
1	495(68,000)	507	12(478)	0.72	530	4
3a	573(72,000)	594	21(617)	0.60	618	29
3b	597(79,000)	653	56(1436)	0.36	670	46
3c	593(88,500)	659	66(1689)	0.31	687	60

^a The numbers in parentheses are the molar extinction coefficient.

^b Stokes shift are calculated from the absorption and emission energies in cm⁻¹ (the numbers in parentheses).

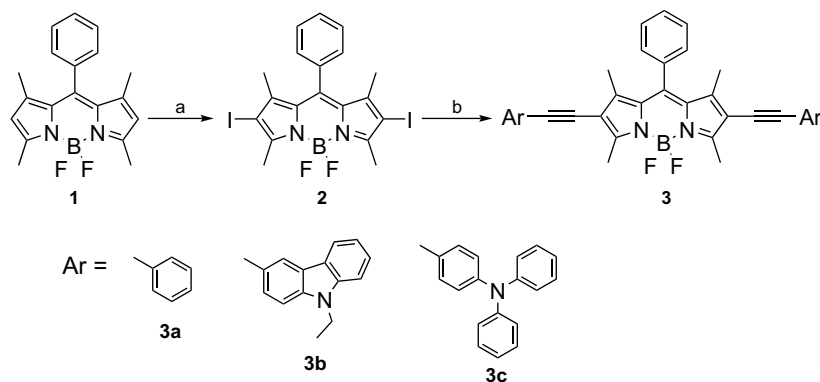
^c Fluorescence quantum yield.

^d The emission wavelength by two-photon excitation.

^e Peak two-photon absorptivity in 10⁻⁵⁰ cm⁴ s photon⁻¹ (GM).

Significantly, compounds **3a–3c** show no linear absorption in the wavelength range 700–1000 nm. Therefore, any emission induced by excitation at this wavelength range must be attributed to a multi-photon absorption process. When the solutions are pumped with laser pulses at wavelength of 800 nm, strong fluorescence emission can be detected. The emission wavelengths of the two-photon induced fluorescence peak for **3a–3c** are 618, 670, and 687 nm, respectively, which show remarkable bathochromic shifts compared with the one-photon induced fluorescence.¹⁴ The red shifts are attributed to the re-absorption of the fluorescence under the concentration solution conditions. A set of SPA (single-photon absorption), SPEF (single-photon excited fluorescence), and TPEF (two-photon excited fluorescence) spectra of **3b** is shown in Figure 2d, in which the shorter wavelength region of the TPEF band partially overlaps with the tail of the linear absorption peak to effect the re-absorption. It is worthy to notice that the TPEF wavelengths of **3b** and **3c** are above 670 nm (in body's therapeutic windows 650–800 nm, low absorptivity region in typical mammalian tissues) with acceptable fluorescence quantum yields, which are significant for bioimaging applications based on TPEF.¹⁵

Taking compound **3b** as an example, as shown in Figure 2, the output intensity of two-photon excited fluorescence is linearly dependent on the square of the input laser intensity, indicating the occurrence of two-photon absorption. The Z-scan data of **3b** in THF, measured in a 1 mm cell with 1.3 μ J pulse energy, were recorded. It showed deep dip typical of nonlinear absorption, which was also an evidence for the occurrence of nonlinear process. The TPA cross sections of compounds **3a–3c** have been measured by open aperture Z-scan experiments performed with a femtosecond (fs) laser source. The values are 29, 46, and 60, respectively, increasing upon the different strength of the electron-donating groups.



Scheme 1. The synthetic routes to compounds **3a–3c**. (a) NIS (2.5 equiv), I₂ (0.5 equiv), ethanol, 90%; (b) alkyne (2.5 equiv), Pd(PPh₃)₄, CuI, THF/NEt₃ 5:1, 60 °C, 68–75%.

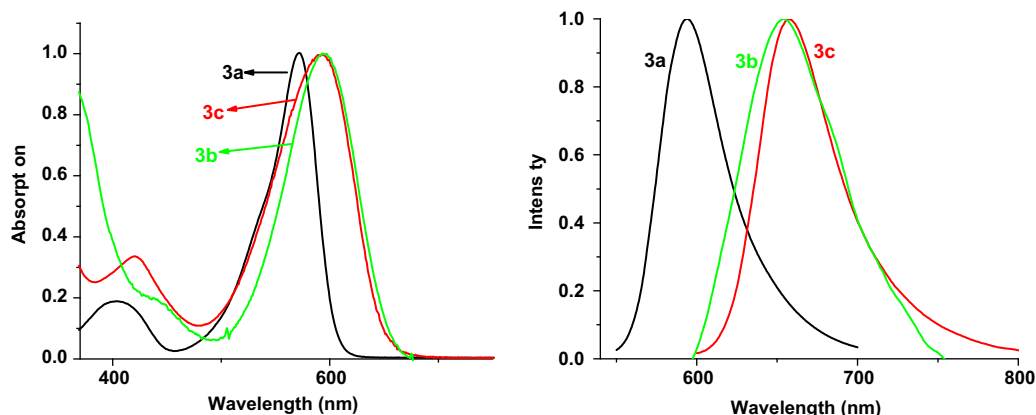


Figure 1. Normalized one-photon absorption (left) and emission (right) spectra of 3a–3c in THF.

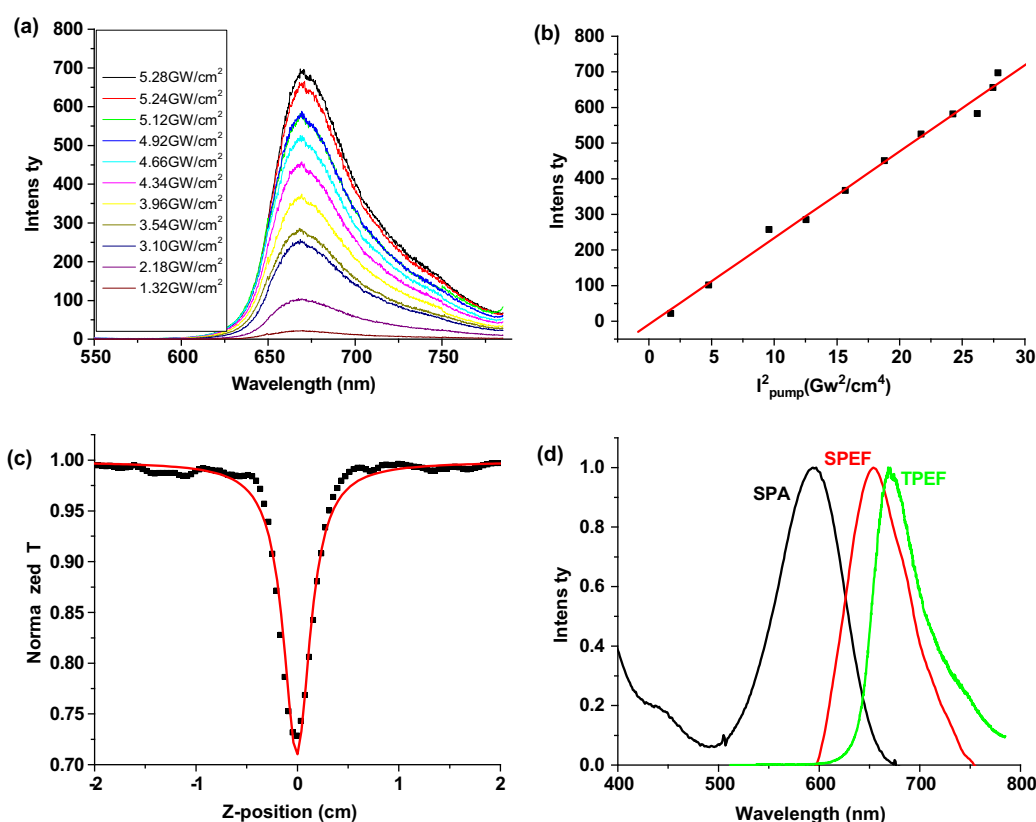


Figure 2. (a) The fluorescence emission spectra of compound **3b** in THF at different laser intensities. (b) The linear dependence of peak fluorescence intensity on the square of the excitation intensity. (c) Z-scan experimental data of compound **3b** in THF (10^{-2} M). The solid lines represent theoretical parameters. (d) Normalized SPA-SPEF-TPEF spectra of **3b** in THF.

For deeper investigating, the electronic states of compounds **3a**–**3c** are studied through cyclic voltammetry and theoretical calculation (B3LYP, 6 31G), and the results are summarized in Table 2. The analysis of the oxidation potentials for **3a**–**3c** (+810, +600, and +470 mV, respectively, in CH_2Cl_2) shows that the carbazole group is a weaker donor than the triphenylamine group, as a consequence, the HOMO (highest occupied molecular orbital) of **3b** is actually located at lower energy than that of **3c**. The stronger electron donating group would result in more intensive ICT process, which is an important factor for the difference of the cross sections. The theoretical calculation shows the same tendency of the charge transfer process as the CV studies, and the related description is in Supplementary data.

For compounds **3b** and **3c**, fluorescence images of MCF 7 (breast cancer) cells are shown in Figure 3. It showed a clear red

Table 2
Electronic state studies of compounds **3a–3c**

Compound	E_g^a [eV]	$E_{\text{onset}}^{\text{ox}b}$	E_p^{ox}	$E_p^{\text{red}c}$	HOMO/LUMO ^d [eV]
3a	2.11	0.81	1.00	−1.30	−5.21/−3.10
3b	1.92	0.60	0.76	−1.32	−5.00/−3.08
3c	1.89	0.47	0.64	−1.42	−4.87/−2.98

^a Energy band gap, determined from UV–vis absorption spectra.

^b $E_{\text{onset}}^{\text{ox}}$ onset oxidation potential; E_p^{ox} oxidation peak potential; potentials reported versus ferrocene as internal standard, glassy carbon working electrode, Ag/AgNO₃ reference electrode, platinum counter electrode, 0.1 M Bu₄NPF₆/CH₂Cl₂, scan rate 100 mV s^{−1} at 20 °C.

^c E_p^{red} reduction peak potential.

^d HOMO $E_{\text{onset}}^{\text{ox}}+4.4$ eV; LUMO HOMO− E_g eV.

intracellular fluorescence, which suggested that **3b** and **3c** were cell permeable. The cells remained viable and no apparent toxicity and

side effects were observed throughout the imaging experiments (about 0.5–1 h). The cell imaging experiment together with their fluorescence properties (emit in the optical windows and acceptable quantum yields) indicate that compounds **3b** and **3c** could be competitive candidates for biological imaging. The fluorescence images were observed under single photon excitation¹⁶ and recorded by Nikon 2200 5 fluorescence microscopy. If we connected acceptors to the dyes, we will obtain some chemosensors to detect heavy metal ions even by two-photon excitation. These works are underway.

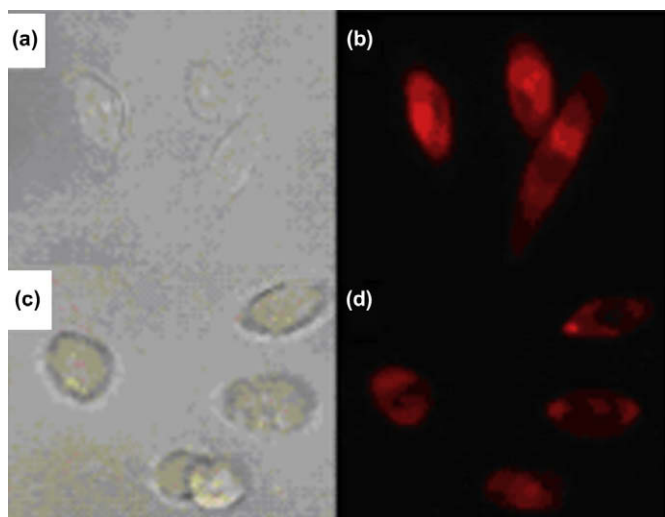


Figure 3. (a) and (c): Bright-field transmission image of MCF-7 cells. (b) MCF-7 cells incubated with **3b** (5 μL , $10^{-5} \text{ mol L}^{-1}$). (d): MCF-7 cells incubated with **3c**. Fluorescence images of MCF-7 cells with **3b** and **3c** (λ_{ex} 488 nm).

3. Summary

In conclusion, by Sonogashira coupling reactions, we have synthesized two novel BODIPY dyes with long absorption and emission wavelengths. The experimental data approved that the compounds were two-photon absorption active materials also with good linear optical properties. The preliminary fluorescence imaging experiments indicated their cell permeability and nontoxicity. Other relative research on increasing the cross sections and fluorescence quantum yields based on this platform are in process.

4. Experimental

4.1. General

The 400 (^1H) MHz NMR and 100 (^{13}C) MHz NMR spectra were measured at room temperature on a Bruker 400 MHz spectrometers using perdeuterated solvents as internal standard: δ (H) in parts per million relative to residual protonated solvent; δ (C) in parts per million relative to the solvent. Melting points were obtained with a capillary melting point apparatus in open-ended capillaries and are uncorrected. Chromatographic purification was conducted with silica gel.

Absorption spectra were recorded on an US HP8453 UV Visible absorption spectrometer and emission spectra were recorded by using a PTI 700 instrument. All studies were made at 20 °C. Excitation and emission spectra were fully corrected by reference to a standard lamp. Solutions were deoxygenated by purging with dried argon prior to recording the spectrum. The reference systems used were Rhodamine B in methanol (ϕ 0.69).

Electrochemical studies made use of cyclic voltammetry with a conventional three-electrode system using a BAS 100 W electrochemical analyzer in deoxygenated and anhydrous CH_2Cl_2 at room

temperature. The potentials are reported versus ferrocene as an internal standard and potentials are calculated relative to SCE assuming $E_{1/2}(\text{Fc}/\text{Fc}^+) + 0.38 \text{ V}$ (ΔE_p 70 mV) versus SCE using a scan rate of 100 mV s^{-1} , glassy carbon working electrode, Ag/AgNO₃ reference electrode, platinum counter electrode, and the sample solutions contained $1.0 \times 10^{-3} \text{ M}$ sample and 0.1 M tetrabutylammonium hexafluorophosphate as a supporting electrolyte. Argon was bubbled for 10 min before each measurement.

For the study on the nonlinear optical properties of these new materials, we employed a femtosecond laser system consisting of a mode-locked Ti:sapphire oscillator (Tsunami, Spectra Physics) and a regenerative amplifier (spitfire). The average output power was about 300 mW with the repetition rate of 1 kHz, the pulse duration of 140 fs, and the wavelength at 800 nm. We used the open-aperture Z-scan technique to measure the TPA cross section. The laser beam with 1.3 μJ pulse energy was focused on the solution in a 1 mm cell by a lens of 10 cm focal length and the transmitted light, after the sample was collected by a photodiode detector connected with a Lock-in amplifier.

MCF-7 cells were cultured in 1640 supplemented with 10% FCS. MCF-7 cells were seeded on 18 mm glass coverslips. After 12 h, the MCF-7 cells were incubated with 5 μL dyes for 0.5 h at room temperature and then washed with phosphate buffered saline (PBS) three times. The glass coverslips were attached to slide before imaging. Fluorescence imaging of intracellular was observed under Nikon 2200 5 fluorescence microscopy. Excitation wavelength of laser was 488 nm.

4.1.1. 2,6-Diido-1,3,5,7-tetramethyl-8-phenyl-4,4-difluoroboradiazaindacene (2). To a solution of 1,3,5,7-tetramethyl-8-phenyl-4,4-difluoroboradiazaindacene (**1**, 170 mg, 0.51 mmol) in anhydrous CH_2Cl_2 (25 mL) was added excess NIS (459 mg, 2.04 mmol). The mixture was stirred at room temperature until total consumption of the starting material (1.5 h, as monitored by TLC). Crude product was then concentrated under vacuum, and purified by silica gel column chromatography (hexane/ CH_2Cl_2 , 2:1). The red-colored fraction was collected and the solvent was removed under reduced pressure to yield the desired compound. Yield: 205 mg (70%); mp 194.3–194.9 °C. ^1H NMR (400 MHz, CDCl_3): 1.37 (s, 6H, CH_3), 2.56 (s, 6H, CH_3), 7.15–7.20 (m, 2H, Ar H), 7.42–7.48 (m, 3H, Ar H). IR (KBr) 3435, 2922, 1530, 1464, 1121, 931 cm^{-1} . TOF MS EI^+ calcd for $\text{C}_{19}\text{H}_{17}\text{BF}_2\text{I}_2\text{N}_2$ 575.9542, found 575.9543.

4.1.2. 2,6-Di(phenylacetylenyl)-1,3,5,7-tetramethyl-8-phenyl-4,4-difluoroboradiazaindacene (3a). Prepared according to the general procedure with phenylacetylene (54.5 μL , 0.497 mmol), **2** (100 mg, 0.207 mmol) in DMF (4 mL). Complete consumption of the starting material was observed after 6 h. The chromatography was performed on silica (CH_2Cl_2 /hexane, 1:2), the purple-colored fraction was collected to get the compound. Yield: 71 mg (76%); mp 330–332 °C. ^1H NMR (400 MHz, CDCl_3): 7.65–7.67 (d, 4H, Ar H), 7.52–7.53 (m, 4H, Ar H), 7.35–7.37 (m, 3H, Ar H), 7.26–7.30 (d, 4H, Ar H), 2.55 (s, 6H, CH_3), 1.35 (s, 6H, CH_3). ^{13}C NMR (100 MHz, CDCl_3): δ 158.4, 144.0, 142.5, 134.5, 131.3, 129.4, 128.4, 128.1, 127.8, 123.4, 116.2, 96.5, 81.6, 13.7, 13.4. TOF MS EI^+ calcd for $\text{C}_{35}\text{H}_{27}\text{BF}_2\text{N}_2$ 524.2235, found 524.2235.

4.1.3. 2,6-Di(9-ethyl-9H-carbazole-3-ethynyl)-1,3,5,7-tetramethyl-8-phenyl-4,4-difluoroboradiazaindacene (3b). Prepared according to the general procedure with 9-ethyl-9H-carbazole-3-ethyne (110 mg, 0.497 mmol), **2** (100 mg, 0.207 mmol) in DMF (4 mL). Complete consumption of the starting material was observed after 8 h. The chromatography was performed on silica (CH_2Cl_2 /hexane, 1:1). The green-colored fraction was collected to get the compound. Yield: 118 mg (75%); mp 241–242 °C. ^1H NMR (400 MHz, CDCl_3): 8.06–8.24 (m, 4H, Ar H), 7.51–7.58 (m, 4H, Ar H), 7.42–7.48 (m, 4H,

Ar H), 7.32 7.36 (m, 3H, Ar H), 7.18 7.22 (m, 4H, Ar H), 4.24 4.38 (q, 4H, N CH₂), 2.78 (s, 6H, CH₃), 1.58 (s, 6H, CH₃), 1.42 1.52 (t, 6H, CH₃). ¹³C NMR (100 MHz, CDCl₃): δ 155.4, 147.6, 146.5, 141.8, 141.2, 138.4, 137.0, 136.2, 134.5, 132.6, 131.5, 131.0, 129.7, 128.1, 126.8, 125.7, 125.1, 123.6, 122.4, 121.7, 116.2, 96.2, 81.8, 37.8, 16.2, 14.7, 13.8. TOF MS EI⁺ calcd for C₅₁H₄₁BF₂N₄ 758.3392, found 758.3387.

4.1.4. 2,6 Di (4 N,N diphenyl phenylacetylenyl) 1,3,5,7 tetramethyl 8 phenyl 4,4 difluoroboradiazaindacene (3c). Prepared according to the general procedure with *N* (4 ethynylphenyl) *N* phenyl benzenamine (134 mg, 0.497 mmol), **2** (100 mg, 0.207 mmol) in DMF (4 mL). Complete consumption of the starting material was observed after 12 h. The chromatography was performed on silica (CH₂Cl₂/hexane, 3:2). The green colored fraction was collected to get the compound. Yield: 121 mg (68%); mp 258–259 °C. ¹H NMR (400 MHz, CDCl₃): 7.42 7.52 (m, 6H, Ar H), 7.35 7.38 (m, 6H, Ar H), 7.22 7.30 (m, 6H, Ar H), 7.00 7.18 (m, 15H, Ar H), 2.68 (s, 6H, CH₃), 1.26 (s, 6H, CH₃). ¹³C NMR (100 MHz, CDCl₃): δ 156.7, 148.0, 147.3, 142.1, 141.4, 138.2, 137.8, 134.1, 133.8, 132.4, 129.6, 128.6, 127.4, 125.0, 123.5, 122.7, 116.5, 96.5, 80.9, 14.8, 13.9. TOF MS EI⁺ calcd for C₅₉H₄₅BF₂N₄ 858.3705, found 858.3709.

Acknowledgements

This work was supported by National Natural Science Foundation of China (No. 20572012, 20876022, 20536010, 10674031) and Program for Changjiang Scholars and Innovative Research Team in University (IRT0711).

Supplementary data

Supplementary data associated with this article can be found in the online version, at doi:10.1016/j.tet.2009.08.002.

References and notes

- (a) Fu, G.; Yang, H.; Wang, C.; Zhang, F.; You, Z.; Wang, G.; He, C.; Chen, Y.; Xu, Z. *Biochem. Biophys. Res. Commun.* **2006**, *346*, 986–991; (b) Wandelt, B.; Cywinski, P.; Darling, G.; Stranix, B. R. *Biosens. Bioelectron.* **2005**, *20*, 1728–1736; (c) Fang, X.; Li, J.; Perlette, J.; Tan, W.; Wang, K. *Anal. Chem.* **2000**, *72*, 747A–753A.
- (a) König, K. J. *Microsc.* **2000**, *200*, 83–104; (b) Aita, K.; Temma, T.; Kuge, Y.; Saji, H. *Luminescence* **2007**, *22*, 455–461; (c) Thomas, D.; Tovey, S. C.; Collins, T. J.; Bootman, M. D.; Berridge, M. J.; Lipp, P. *Cell Calcium* **2000**, *28*, 213–223; (d) Grapengiesser, E. *Cell Struct. Funct.* **1993**, *18*, 13–17.
- Fabian, J.; Nakazumi, H.; Matsuoka, M. *Chem. Rev.* **1992**, *92*, 1197–1226.
- (a) Denk, W.; Strickler, J. H.; Webb, W. W. *Science* **1990**, *248*, 73–76; (b) Wang, X.; Krebs, L. J.; Al-Nuri, M.; Pudavar, H. E.; Ghosal, S.; Liebow, C.; Nagy, A.; Schally, A. A. W.; Prasad, P. N. *Proc. Natl. Acad. Sci. U.S.A.* **1999**, *96*, 11081–11084; (c) Köhler, R. H.; Cao, J.; Zipfel, W. R.; Webb, W. W.; Hansen, M. R. *Science* **1997**, *276*, 2039–2042.
- (a) He, G. S.; Tan, L.-S.; Zheng, Q.; Prasad, P. N. *Chem. Rev.* **2008**, *108*, 1245–1330; (b) Prasad, P. N. *Introduction to Biophotonics*; Wiley: New York, NY, 2003; (c) Albota, M.; Beljonne, D.; Brédas, J.; Ehrlich, J. E.; Fu, J.; Heikal, A. A.; Hess, S. E.; Kogej, T.; Levin, M. D.; Marder, S. R.; McCord-Maughon, D.; Perry, J. W.; Röckel, H.; Rumi, M.; Subramaniam, G.; Webb, W. W.; Wu, X.-L.; Xu, C. *Science* **1998**, *281*, 1653–1656.
- (a) Kato, S.-I.; Matsumoto, T.; Shigeiwa, M.; Gorohmaru, H.; Maeda, S.; Ishi-i, T.; Mataka, S. *Chem. Eur. J.* **2006**, *12*, 2303–2317; (b) Picot, A.; D'Aléo, A.; Baldeck, P. L.; Grishine, A.; Duperray, A.; Andraud, C.; Maury, O. *J. Am. Chem. Soc.* **2008**, *130*, 1532–1533; (c) Margineanu, A.; Hofkens, J.; Cotlet, M.; Habuchi, S.; Stefan, A.; Qu, J.; Kohl, C.; Müllen, K.; Vercammen, J.; Engelborghs, Y.; Gensch, T.; De Schryver, F. C. *J. Phys. Chem. B* **2004**, *108*, 12242–12251; (d) Brousmiche, D. W.; Serin, J. M.; Fréchet, J. M. J.; He, G. S.; Lin, T.-C.; Chung, S.-J.; Prasad, P. N.; Kannan, R.; Tan, L.-S. *J. Phys. Chem. B* **2004**, *108*, 8592–8600; (e) Qu, J.; Kohl, C.; Pottek, M.; Müllen, K. *Angew. Chem., Int. Ed.* **2004**, *43*, 1528–1531.
- (a) Brousmiche, D. W.; Serin, J. M.; Fréchet, J. M. J.; He, G. S.; Lin, T.-C.; Chung, S.-J.; Prasad, P. N.; Kim, K.-S.; He, G. S.; Swiatkiewicz, J.; Prasad, P. N.; Baker, G. A.; Bright, F. V. *Chem. Mater.* **2001**, *13*, 4071–4076.
- (a) Atilgan, S.; Ekmekci, Z.; Lale Dogan, A.; Güc, D.; Akkaya, E. U. *Chem. Commun.* **2006**, 4398–4400; (b) Matsumoto, T.; Urano, Y.; Shoda, T.; Kojima, H.; Nagano, T. *Org. Lett.* **2007**, *9*, 3375–3377.
- (a) Haugland, R. P. *Handbook of Fluorescent Probes and Research Chemicals*, 6th ed.; Molecular Probes: Eugene, OR, 1996; (b) Loudet, A.; Burgess, K. *Chem. Rev.* **2007**, *107*, 4891–4932; (c) Ulrich, G.; Ziessel, R.; Harriman, A. *Angew. Chem., Int. Ed.* **2008**, *47*, 1184–1201; (d) Ziessel, R.; Ulrich, G.; Harriman, A. *New J. Chem.* **2007**, *31*, 496–501.
- (a) Porrès, L.; Mongin, O.; Blanchard-Desce, M. *Tetrahedron Lett.* **2006**, *47*, 1913–1917; (b) Nicolini, C.; Baranski, J.; Schlummer, S.; Palomo, J.; Lumbierres-Burgues, M.; Kahms, M.; Kuhlmann, J.; Sanchez, S.; Gratton, E.; Waldmann, H.; Winter, R. *J. Am. Chem. Soc.* **2006**, *128*, 192–201; (c) Zhang, Q.; Xu, G.; Prasad, P. N. *Chem. Eur. J.* **2008**, *14*, 5812–5819; (d) Meltola, N. J.; Wahlroos, R.; Soini, A. E. *J. Fluoresc.* **2004**, *14*, 635–647; (e) Meltola, N. J.; Soini, A. E.; Hänninen, P. E. *J. Fluoresc.* **2004**, *14*, 129–138; (f) Bouit, P. A.; Kamada, K.; Feneyrou, P.; Berginc, G.; Toupet, L.; Maury, O.; Andraud, C. *Adv. Mater.* **2009**, *21*, 1151–1154.
- (a) Cakmak, Y.; Akkaya, E. U. *Org. Lett.* **2009**, *11*, 85–88; (b) Zhang, D.; Wen, Y.; Xiao, Y.; Yu, G.; Liu, Y.; Qian, X. *Chem. Commun.* **2008**, 4777–4779.
- (a) Rumi, M.; Ehrlich, J. E.; Heikal, A. A.; Perry, J. W.; Barlow, S.; Hu, Z. Y.; McCord-Maughon, D.; Parker, T. C.; Röckel, H.; Thayumanavan, S.; Marder, S. R.; Beljonne, D.; Brédas, J.-L. *J. Am. Chem. Soc.* **2000**, *122*, 9500–9510; (b) Lee, W.-H.; Cho, M.; Jeon, S.-J.; Cho, B. R. *J. Phys. Chem. A* **2000**, *104*, 11033–11040; (c) Kogej, T.; Beljonne, D.; Meyers, F.; Perry, J. W.; Marder, S. R.; Brédas, J.-L. *Chem. Phys. Lett.* **1998**, *298*, 1–6.
- Ning, Z.; Chen, Z.; Zhang, Q.; Yan, Y.; Qian, S.; Cao, Y.; Tian, H. *Adv. Funct. Mater.* **2007**, *17*, 3799–3807.
- Liu, Z.; Fang, Q.; Cao, D.; Wang, D.; Xu, G. *Org. Lett.* **2004**, *6*, 2933–2936.
- (a) Ghoroghchian, P. P.; Frail, P. R.; Susumu, K.; Blessington, D.; Brannan, A. K.; Bates, F. S.; Chance, B.; Hammer, D. A.; Therien, M. J. *Proc. Natl. Acad. Sci. U.S.A.* **2005**, *102*, 2922–2927; (b) Weissleder, R.; Ntziachristos, V. *Nat. Med.* **2003**, *9*, 123–128.
- Lu, Z.; Wang, P.; Zhang, Y.; Chen, J.; Zhen, S.; Leng, B.; Tian, H. *Anal. Chim. Acta* **2007**, *597*, 306–312.